Magnetoelectric intrinsic gradiometer with high detection sensitivity and ambient noise rejection

Mingji Zhang, Siu Wing Or, and Yiu Man Yip*
Department of Electrical Engineering
The Hong Kong Polytechnic University
Hung Hom, Kowloon, Hong Kong
*Corresponding author: eeswor@polyu.edu.hk

Abstract*—We report theoretically and experimentally the simultaneous realization of high detection sensitivity and high ambient noise rejection in an intrinsic gradiometer based on the giant magnetoelectric effect and the magnetic field gradient sensing technique in two specifically designed and arranged magnetoelectric magnetometers. The output voltage of the gradiometer is directly obtained from the intrinsic difference voltage between the two magnetoelectric magnetometers and is calibrated magnetic field gradient to give a high detection sensitivity of 3.2 mV/(Oe/m) and a high ambient noise rejection of 30 dB (equivalent to a noise level of* $\mathbf{20}$ *pT/*$\sqrt{\boldsymbol{Hz}}$ *at the natural resonance frequency of 120 kHz). The consistent characteristics of the magnetoelectric magnetometers result in almost zero non-linearity between the gradiometer output voltage and its magnetic field gradient over a broad range of frequency from 1 Hz to 170 kHz.*

Keywords*—ambient noise rejection; intrinsic gradiometer; magnetoelectric effect; magnetometer; magnetic field gradient*

I. INTRODUCTION

A gradiometer generally consists of two magnetometers spatially separated by a baseline to measure magnetic field gradient by differencing the output signals of the magnetometers over the baseline for achieving high immunity to both ambient noise and background fields. The gradiometer has been verified as an excellent means for extremely weak magnetic measurements in applications of geomagnetism mapping [1], magnetic source positioning [2], medical diagnosis [3], etc. In these applications, magnetic field noises from ambient and electric field noise from measuring circuits are considered as important factors which limit the measurement accuracy. Gradiometers based on induction effect, hall effect, giant magnetoresistance (GMR), and superconducting quantum interference device (SQUID) have been investigated, implemented, and even commercialized [4] over the past decades. Most of these gradiometers perform real-time differencing by external signal-processing and data acquisition systems, and this is referred to extrinsic differencing. While ambient magnetic field noises can be reduced, electric field noises from measuring circuits are doubled because of the transmission process in cables, especially for high-frequency measurements. We solve this problem by intrinsically difference the magnetometer output inside the magnetometer and directly outputs the differenced voltage signal with respect to magnetic field gradient. Another limitation of above mechanisms are either bulked size, complex modulating system, high maintaining cost or low sensitivity [5]. The magnetoelectric effect engaged in laminated composites is the product effects of magnetostrictive and piezoelectric couplings, numerous previous studies have demonstrate its advantages over other mechanisms [6]. Researches on magnetoelectric gradiometer are limited. The first magnetoelectric gradiometer was implemented and characterized in 2009 based on a transformer structure using Terfenol-D and PMN–PT laminates working near an electromechanical resonance [7, 8]. Although high sensitivity was achieved in this work, the transformer structure requires an external voltage excitation and complex electrodes. Moreover, few data on gradiometer output as a function of magnetic field gradient was presented, which is one of the most important figure of merits of gradiometer. Another type of magnetoelectric gradiometer achieved an overall noise rejection factor of 20 below 10 Hz in a tri–layer Metglas/PZT push-pull structure using a classical differential technique [9]. However, the investigated frequency range is far from power frequency and electromechanical resonance frequency.

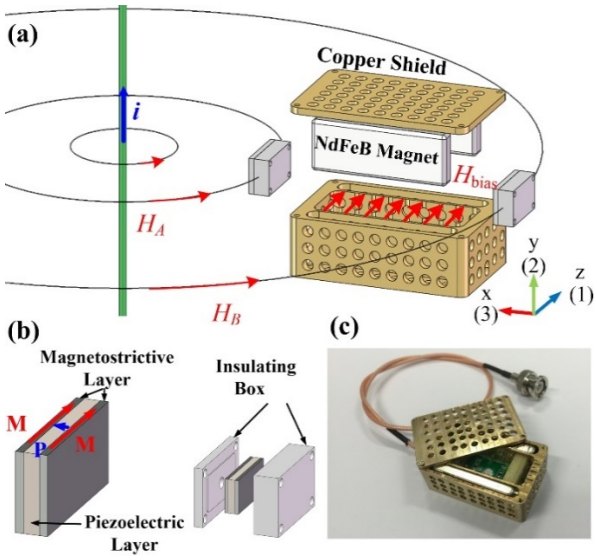

Fig. 1. (a) Assembling and calibration schematics (*x*, *y*, *z* and 1, 2, 3 refer to geometry coordinates and material frame, respectively); (b) Schematic diagram of sensing unit; (c) magnetoelectric gradiometer prototype.

In this study, we creatively report the realization of intrinsic gradiometer based on magnetoelectric magnetometers. As shown in Fig. 1(a), the gradiometer is made of two Terfenol–D/PZT8 laminated composite magnetoelectric magnetometers by orientating their lengths along the magnetic bias field in the *z* direction provided by a pair of NdFeB magnet bars and by separating them with an optimal baseline, *L*=35 mm, in the *x* direction. The copper housing is grounded and drilled with holes in an array form of 3.2 mm diameter to shield electric field noise and reduce the eddy-current effect. Terfenol–D and PZT–8 plates of dimensions 12 mm long, 6 mm wide, and 1 mm thick, with magnetization and polarization shown in Fig. 1(b). Fabrication of magnetoelectric laminated composites are

specified in details in [6]. The two magnetoelectric laminated composites, which externally stress-free insulated by 3D-printed plastic boxes (Fig. 1(b)), are deliberately selected from 10 samples by both static and dynamic characterization to minimize the difference between their voltage coefficients less than 3%. The prototype of the magnetoelectric gradiometer is shown in Fig. 1(c), by internally connecting the negative polarization sides of piezoelectric phase on PCB board, the gradiometer output is obtained by intrinsic voltage differencing at each positive polarization sides of piezoelectric phase through a BNC connector. The combination of the intrinsic differencing technique and giant magnetoelectric effect in magnetoelectric magnetometers as well as the delicated fabrication control guarantee an excellent performance in high sensitivity, high ambient noise rejection, and almost zero non-linearity of proposed gradiometer.

II. Basic Principles

Magnetic field tensor **G** (Oe/m) is vector differential of **H**, with respect to geometric vector **r** (m) as

$$\mathbf{G} = \partial \mathbf{H} / \partial \mathbf{r} \tag{1}$$

In practical, the specific component of **G** can be approximated by spatial difference as

$$G_{ij} = H_{i,A} - H_{i,B} \,/ L_j \; (i,j = x,y,z) \tag{2}$$

where $H_{i,\mathrm{A}}$ and $H_{i,\mathrm{B}}$ are magnetic field in *i*–direction at of sensing points A and B, respectively. L_j is the baseline length in j–direction. When uninform magnetic field is applied to the gradiometer, the voltage response from gradiometer is determined by the coupling effects of magnetostrictive and piezoelectric constitutive relation in [6] as

$$V_{\mathrm{g}}(\omega) = (\alpha\,(\omega) H_{z,A} + n_A) - (\alpha\,(\omega) H_{z,B} + n_B) \tag{3}$$

where $\alpha\,(\omega)$ (V/Oe) is the magnetoelectric voltage coefficient. n_A and n_B are voltage noises of sensing units caused by ambient magnetic field noise, electric field noise, vibration noise and $1/f$ noise[10]. Assuming $n_A = n_B$ results in gradiometer sensitivity $S_{g,ij}$ (V/Oe/m) expression as

$$S_{g,ij} = \mathrm{d}V_{\mathrm{g}} / \mathrm{d}G_{ij} = \alpha\,(\omega) * L \tag{4}$$

The performance of ambient noise reducing is evaluated by noise reduction ratio (NRR) defined as

$$NRR = -20\log[2 * N_G(\omega) / (N_A(\omega) + N_B(\omega))] \tag{5}$$

where $N_G(\omega)$, $N_A(\omega)$, and $N_B(\omega)$ in unit of $(\mathrm{V}/\sqrt{\mathrm{Hz}})$ are voltage noise floor of magnetoelectric gradiometer and sensing units A and B, respectively.

III. Experiments Results and Discussion

As shown in Fig. 1(a), the magnetoelectric gradiometer sensitivity S_g was calibrated by fixing gradiometer in *x*–*z* plane and a straight cable in *y* direction so that each sensing unit is tangent to the circumferential magnetic field generated by cable. The distance from sensing units to cable were fixed to be 15 mm and 50 mm, respectively. Gradiometer sensitivity S_g was obtained by controlling the current in the cable (root mean square (RMS) value) from 0 to 6 A corresponding to G_{zx} from 0–16 Oe/m at each frequency. The magnetoelectric gradiometer output voltage was measured by a lock–in amplifier (SR865). Results in Fig. 2 shares the similar spectrum to α spectrum in, which can be explained magnetoelectric resonance effect. An overall S_g of 0.4 mV/(Oe/m) is achieved over broad frequency range up to 170 kHz, among which, maximum S_g of 3.2 mV/(Oe/m) is obtained at resonance frequency of 120 kHz.

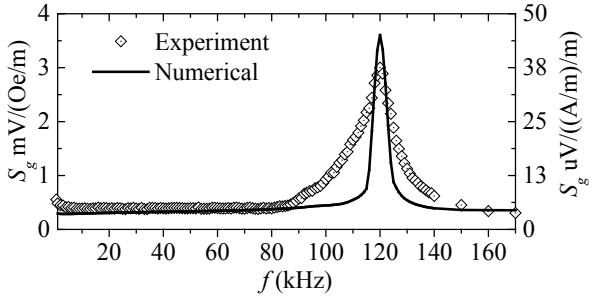

Fig. 2. Magnetoelectric gradiometer sensitivity S_g spectrum.

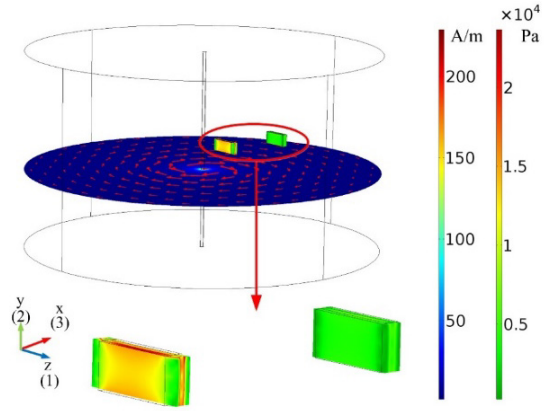

Fig. 3. Numerical results of stress (Pa) and magnetic field (A/m) distribution of gradiometer sensitivity calibration process modelling results at 1 kHz.

The calibration of S_g was numerically modeled following the experiment configuration in Fig. 1(a). Results in Fig. 3 illustrate the magnetic field generated by straight cable and induce von Mises stress in magnetoelectric gradiometer when cable is excited by 1 A (rms value) current at 1 kHz. We see from Fig. 3 that the sensing unit subjects to larger magnetic field have larger deformation and stress, resulting in larger output voltage governed by right hand terms in (3). It is interesting to find in inset figure in Fig. 3 that a small bended deformation appears due to magnetic field component (H_x) transverse to the sensitive axis (z) of magnetoelectric gradiometer. The reasons for small bended deformation are L–T mode dominant vibration due to structure and anisotropic magnetostrictive properties of Terfenol–D plates. Parametric sweep of cable current excitation among 0–6 A (rms value) is conducted at each frequency. Numerical results of S_{g} spectrum in Fig. 2 have the similar trend as α spectrum in [6], suggesting that S_{g} is physically determined by α of each sensing units as expressed in (4).

The magnetoelectric gradiometer output voltage as function of G_{zx} was calibrated experimentally. Results in Fig. 4 shows V_g as function of G_{zx} at critical frequencies of 50 Hz, 10, 120, and 160 kHz corresponding to the S_g spectrum in Fig. 2. Perfect linear V_g responses to G_{zx} over a broad frequency range from 1 Hz to 170 kHz is obtained.

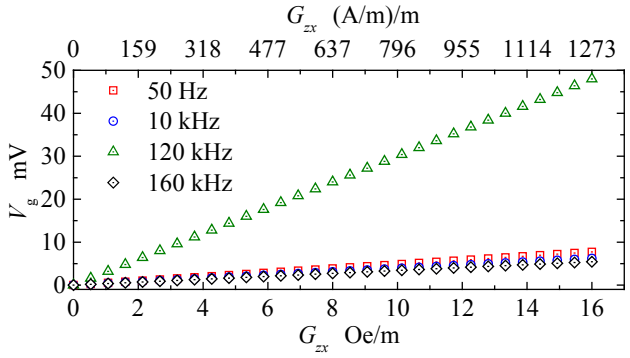

Fig. 4. Magnetoelectric gradiometer sensitivity calibration results: V_g as a function of Gzx

The equivalent magnetic field noise was measured by a lockin amplifier (RS865). Noise reduction ratio, NRR, is evaluated using (5). Results in Fig. 5 demonstrate that an average of 10 dB NRR is achieved from 1 Hz to 1 kHz, among which maximum NRR 27 dB is obtained at 10 Hz. The 3-dB cutoff frequency is 3 kHz. High frequency NRR is limited because of noise phase lag in each magnetometer. Fig. 5 suggests that below the cutoff frequency, namely from 1 Hz to 3 kHz, a minimum equivalent magnetic noise of 2×10^{-7} Oe/ $\sqrt{\text{Hz}}$ can be achieved, corresponding to equivalent magnetic flux density noise of 20 pT/$\sqrt{\text{Hz}}$.

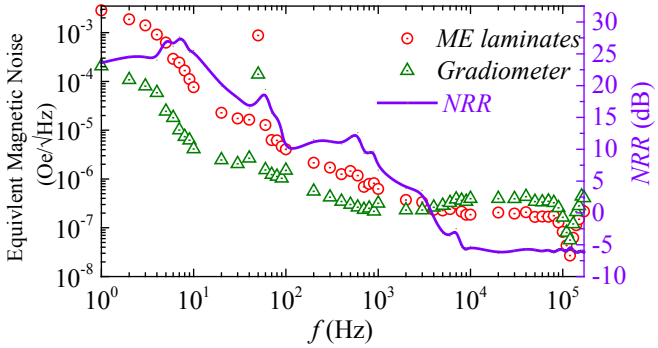

Fig. 5. Equivalent magnetic field noise floor of magnetoelectric magnetometers and magnetoelectric gradiometer and noise reduction ratio of magnetoelectric gradiometer.

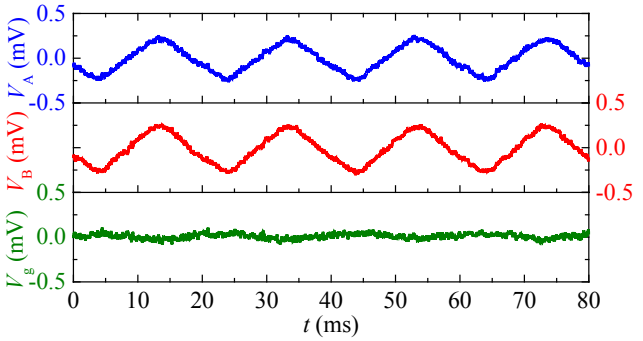

Fig. 6.Voltage output waveform of magnetoelectric magnetometers and magnetoeelctric gradiometer.

Considering the fact that the power frequency noise is one of the predominant noise type when magnetoelectric magnetic sensor is applied in industrial environment, the ambient noise reduction performance is tested by artificially created by exciting line cable with current of 12 A (RMS value) 1.8 m away from gradiometer. The voltage outputs V_A, V_B and V_g are simultaneously recorded by oscilloscope (MSO 2014, Tektronix) with its internal 60 kHz low–pass filter. Results in Fig. 6 obviously demonstrates the ambient noise rejection performance of propose magnetoelectric gradiometer, the ambient power frequency noise is approximately 12 times rejected in the present test.

IV. Conclusion

We have developed intrinsic magnetic field gradiometer based on magnetoelectric magnetometers. The proposed magnetometer has been theoretically analyzed, and practically prototyped and experimentally tested. It has almost zero nonlinearity and overall sensitivity 0.5 mV/Oe/m over broad frequency range from 1 Hz to 170 kHz. High sensitivity up to 3.2 mV/(Oe/m) is achieved at resonance frequency at 120 kHz. A 10 dB overall noise rejection rate is achieved over broad frequency range from quasi-static to 1 kHz. Together with conventional noise rejection techniques (such as filter, lock-in or low noise amplifier optimization), it is possible to obtain 10^2 fT/$\sqrt{\text{Hz}}$ scale ultralow noise magnetic field sensor based on magnetoelectric gradiometer.

Acknowledgments

This work was supported in part by the Research Grants Council of the Government of the Hong Kong Special Administrative Region under Grant No. 522813 and in part by The Hong Kong Polytechnic University under Grant No. RTUY.

References

[1] M. Schneider, S. Linzen, M. Schiffler, E. Pohl, B. Ahrens, S. Dunkel, R. Stolz, J. Bemmann, H. G. Meyer, and D. Baumgarten, "Inversion of Geo-Magnetic SQUID Gradiometer Prospection Data Using Polyhedral Model Interpretation of Elongated Anomalies," *Ieee Transactions on Magnetics,* vol. 50, no. 11, Nov, 2014.

[2] T. Nara, and W. Ito, "Moore-Penrose generalized inverse of the gradient tensor in Euler's equation for locating a magnetic dipole," *Journal of Applied Physics,* vol. 115, no. 17, May 7, 2014.

[3] J. E. McGary, "Real-Time Tumor Tracking for Four-Dimensional Computed Tomography Using SQUID Magnetometers," *IEEE Transactions on Magnetics,* vol. 45, no. 9, pp. 3351-3361, Sep, 2009.

[4] M. Valentino, C. Bonavolonta, N. Marrocco, G. Peluso, and G. P. Pepe, "Gmr Second Order Electronic Gradiometer as Eddy Current Probe in Nde Applications," *Review of Progress in Quantitative Nondestructive Evaluation, Vols 28a and 28b,* vol. 1096, pp. 350-354, 2009.

[5] P. Ripka, and M. Janosek, "Advances in Magnetic Field Sensors," *Ieee Sensors Journal,* vol. 10, no. 6, pp. 1108-1116, Jun, 2010.

[6] C. M. Leung, "Magnetoelectric smart current sensors for wireless condition monitoring applications," Dept. of Electrical Engineering, Hong Kong Polytechnic University, Hongkong, 2012.

[7] V. Bedekar, R. A. Islam, H. Kim, M. I. Bichurin, S. N. Ivanov, Y. J. Pukinski, and S. Priya, "Magnetoelectric gradiometer," *European Physical Journal B,* vol. 71, no. 3, pp. 387-392, Oct, 2009.

[8] V. Bedekar, M. I. Bichurin, S. N. Ivanov, Y. J. Pukinski, and S. Priya, "Metal-ceramic laminate composite magnetoelectric gradiometer," *Review of Scientific Instruments,* vol. 81, no. 3, Mar, 2010.

[9] Y. Shen, J. Gao, L. Shen, D. Gray, J. Li, P. Finkel, D. Viehland, X. Zhuang, S. Saez, and C. Dolabdjian, "Analysis of the environmental magnetic noise rejection by using two simple magnetoelectric sensors," *Sensors and Actuators a-Physical,* vol. 171, no. 2, pp. 63-68, Nov, 2011.

[10]Y. Wang, D. Gray, D. Berry, J. Gao, J. Li, D. Viehland, and H. Luo, "Equivalent magnetic noise in magnetoelectric Metglas/Pb (Mg1/3Nb2/3) O3 - PbTiO3 laminate composites," *physica status solidi (RRL)-Rapid Research Letters,* vol. 5, no. 7, pp. 232-234, 2011.